Physicochem. Probl. Miner. Process., 57(3), 2021, 21-35

http://www.journalssystem.com/ppmp

Physicochemical Problems of Mineral Processing

ISSN 1643-1049

Received October 10, 2020; reviewed; accepted March 12, 2021

Digital image processing (*DIP*) application on the evaluation of iron-rich heavy mineral concentrates produced from river sand using a sequential mineral processing approach

Mert Terzi [1], Ilgin Kursun Unver [1], Mustafa Cinar [2], Orhan Ozdemir [1]

[1] Istanbul University-Cerrahpasa Mining Engineering Department, Buyukcekmece, Istanbul, Turkey

[2] Canakkale Onsekiz Mart University Mining Engineering Department, Canakkale, Turkey

Corresponding author: orhanozdemir@istanbul.edu.tr (Orhan Ozdemir)

Abstract: In this study, the iron-rich heavy mineral concentrate production from river sand as a by-product of an alternative resource by gravity, magnetic separation, and flotation methods were investigated in detail. For the physical separation of the sample and increasing the Fe_2O_3 content, a shaking table and a wet high-intensity magnetic separator were used, respectively. The gravity and magnetic separation experiments included rougher, cleaner, and scavenger circuits. In the flotation experiments, cationic flotation with ethylenediamine under acidic conditions, and anionic flotation with sodium oleate under alkaline conditions were performed. The iron and silica content of the products obtained were determined by digital image processing (*DIP*) methods and compared with the classical analytical procedures. Finally, a flow chart was proposed for the processing of the ore according to the optimum enrichment parameters were determined from the experiments. The results obtained in this study show that it is possible to produce an iron-rich heavy mineral concentrate with Fe_2O_3 grade and recovery rate of 79.13% and 57.81%, respectively, in addition to a potential feed for the production of quartz sand and feldspar concentrates.

Keywords: gravity separation, magnetic separation, flotation, silica, iron, magnetite

1. Introduction

Silica sand, which is formed by the decomposition of quartz-rich magmatic and metamorphic rocks, is a raw material commonly used in glass, cement, detergent, plastic, ceramic, electronics, paint, casting, and metallurgical industries. In general, it is desired that the SiO_2 content of silica sand used in glass production must be no less than 99%. Silica sands with stable chemical composition and low Fe_2O_3 content (<0.02-0.1%) are generally preferred in glass production. Accordingly, silica sand is subjected to mineral processing to comply with physical or chemical specifications (Kose and Tureli, 1986; Ubaldini et al., 1996; Hacifazlioglu, 2011). Also, the beach and river sediments have been used in glass production. For example, river sediments are rich in silicate minerals like quartz and feldspar. Upgrading river sediments by physical processing methods such as gravity, magnetic, and electric separation methods showed that the silica content of river sediment can be enriched from 60-70% to 94% (Rajib et al., 2009). Rahman et al. (2015) stated that after the separation of heavy minerals from the river sand of Bangladesh, the resulting quartz-rich fraction can be used in glass production. Additionally, it was stated that an iron-rich concentrate (>60%) can be obtained from the same deposit with the physical separation methods.

Iron is the fourth most abundant metal in the Earth's crust after aluminium and the second most abundant metal in general. The main ore minerals of iron are hematite, magnetite, titano-magnetite, goethite, and siderite. Today, in many countries, most of the rich iron ore reserves are depleted and the sustainable production of low-grade iron ores has become a critical debate in the mining industry. For example, magnetite and ilmenite deposits are common in coastal sands. Many such deposits have been

DOI: 10.37190/ppmp/134216

studied as potential sources of iron ore (Christie and Brathwaite, 1997; Liu et al., 2014). Magnetic separation is the most economical and environmentally friendly method used for iron ore processing. However, iron ores need to be enriched using a process suitable according to the properties such as mineral composition, physical properties, and liberation degree between iron-containing/gangue minerals. In the recovery of iron from low-grade iron ore; the application of various methods such as flotation, gravity separation, and magnetic separation has been investigated by many researchers (Li et al., 2010; Seifelnassr et al., 2013; Filippov et al., 2014).

Traditionally high precision multi-element analysis has been performed in analytical laboratories on the ore samples using standard techniques such as X-ray fluorescence (*XRF*) and Inductively coupled plasma (*ICP*) spectroscopies. These analyzes typically provide data that can lag the production of the mine or plant due to intensive sample preparation (Endo and Sakao, 1980; Death et al., 2008). These traditional techniques have also been used for iron ore analysis (Bhargava, 2006). In addition to the abovementioned disadvantages such as extended sample preparation durations, these techniques, especially wet chemical analysis methods that require the use of strong acids at the digestion step, have the potential to pollute the environment (Sheng et al., 2015).

Digital image processing (*DIP*) is the use of computer algorithms to perform image processing on digital images. The high flexibility of the *DIP* methods makes it useful in a wide variety of processes (Billingsley, 1970; Cao, 2006). Therefore, such methods are used in many disciplines including medicine, geodesy, photogrammetry, earth sciences, chemistry, astrophysics, biotechnology, and metallurgy (Maras et al., 2010). Moreover, the *DIP* method has been used for the evaluation of several processes such as flotation (Moolman et al., 1994; Aldrich et al., 2010), particle size distribution analysis (Kursun, 2009), and solid-liquid separation (Stanford et al., 1992) in the mineral processing discipline. Alternatively, these methods have also been researched in several studies as an alternative to traditional techniques used in ore grade analyzes (Singh and Rao, 2006; Khorram et al., 2011; Perez et al., 2011).

In this context, this study aimed to investigate the possibility of iron concentrate production from silica-rich river sediment with high iron content by gravity, magnetic separation, and flotation methods. Moreover, the application of the digital image processing methods as an alternative to classical analytical analysis methods in determining the iron and silica content of the products obtained was evaluated and discussed in detail. Finally, a flow chart was proposed for a possible scale-up ore processing based on the optimum parameters.

2. Materials and methods

2.1. Materials

The Silica-rich river sediment sample used in the study was obtained from the Canakkale region, Turkey. In the characterization studies; the physical, chemical, and mineralogical properties of the samples were determined by particle size distribution analysis (*PSD*), chemical analyzes by inductively coupled plasma mass spectrometry (*ICP-MS*) method, X-ray diffraction (*XRD*) analyzes, and optical microscope investigations on the representative samples. The *PSD* and optical microscopy analyzes were performed on the original samples. On the other hand, the samples were reduced to -75 μm particle size using an agate grinder for instrumental analyzes such as ICP and *XRD* methods. ICP-MS analyzes were carried out using Perkin Elmer Nexion 2000 to determine the major oxide contents of the sample. Lithium tetraborate ($Li_2B_4O_7$) fusion and nitric acid digestion methods were used for the preparation of the samples for *ICP* analyzes. The results of the chemical analysis of the sample are presented in Table 1. As a result of chemical analysis, SiO_2 and Fe_2O_3 contents of the sample were determined as 59.16% and 6.82%, respectively. Accordingly, the sample was identified as a silica-rich ore with considerable iron content.

The *PSD* analysis of the sample was performed under TS 3530 EN 933-1 standard by using Retsch AS200 Basic sieve shaker and Impact brand ISO3310-1: 2000 test sieve series. The d_{80} and d_{50} sizes of the sample were determined as 867 μm and 364 μm, respectively (Fig. 1a). To describe the minerals in the samples, *XRD* analyzes and mineralogical examinations were carried out. *XRD* analyzes were performed using GNR APD 2000 Pro X-ray diffractometer, and the measurements were realized under Cu-Kα radiation at 40 kV voltage and 30 mA

Table 1. Major oxide contents of the sample

Oxides	Assay Values (%)	Oxides	Assay Values (%)
Al_2O_3	18.82	Na_2O	4.55
Fe_2O_3	6.82	P_2O_5	Not Detected
K_2O	1.43	SiO_2	59.16
CaO	3.89	TiO_2	0.80
MgO	0.72	LOI*	2.15
MnO	0.15	Total	98.49

*Loss in ignition

current with a goniometer velocity of 2θ = 1° / min. The obtained *XRD* spectra were evaluated using Philips Xpert Highscore software. A trinocular microscope (SOIF BK-POL) was used for the optical examination and imaging studies. As seen in Fig. 1b, thedominant mineral in the sample was quartz, mostly colorless but also observed in different colors. Iron content is mainly attributed to magnetite mineral which is partly free and partly locked with quartz particles. Additionally, ilmenite and titanomagnetite were identified as secondary iron-containing minerals. On the other hand, kaolinite and albite minerals, which have lost their euhedral forms as a result of decomposition, were secondary in the sample. Trace amounts of mica, rutile, and apatite minerals were also observed. It was determined that the minerals in the sample did not accumulate in a certain fraction and showed a relatively homogeneous distribution. However, it was found that the degree of liberalization, especially in terms of quartz and magnetite, increased after the particle size of 125 µm. Additionally, the presence of cemented structures with quartz and magnetite content having low breakage resistance was observed especially in the fractions coarser than 1 mm.

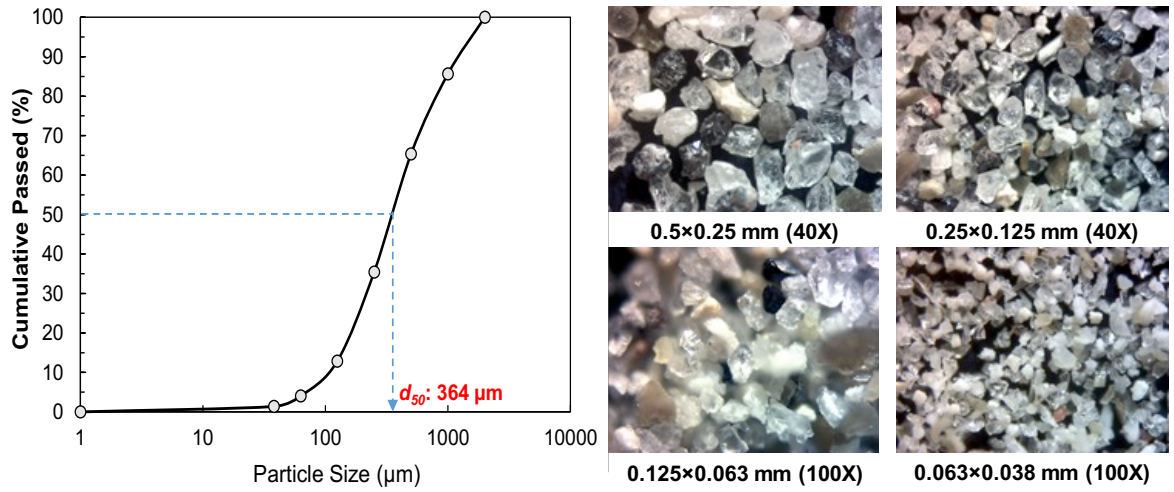

Fig. 1. (a) *PSD* results of the original sample, (b) Optical microscope images of different size fractions

2.2. Methods

2.2.1. Sample preparation

According to the results of the mineralogical examination, the studies for the sample preparation were carried out for examining the conditions of breaking the cemented structures observed in the +1 mm fraction, besides, to obtain narrow particle size fractions suitable for the gravity and magnetic separation experiments. The particles, coarser than 8 mm, were removed initially as they were not related to the general mineralogical composition of the sample due to the transportation of pebble-sized particles at the river bed. Subsequently, the remained sample was crushed to -1 mm using a roll crusher (Unal Engineering, Turkey) in a closed circuit. The resulting sample was subjected to scrubbing to break free the cemented structures and clean the particle surfaces from the potential contaminations. The effect of scrubbing was investigated for 1, 5, and 10 min under constant conditions of 1000 rpm of mixing speed and 50% solids. After the scrubbing, the sample was classified into 3 different size groups, namely 1×0.5,

0.5×0.212, and 0.212×0.038 mm. Since the -0,038 mm fraction was out of the particle size range that could be enriched effectively with the physical enrichment devices used within the scope of the study, it was not included in the enrichment studies.

2.2.2. Pre-processing with gravity and magnetic separation methods

As the first step of enrichment experiments, it was decided to examine the pre-processing of the sample by gravity separation considering the density differences between magnetite and gangue minerals and the relatively coarse (~125 μm) liberation size of the particles. As mentioned in Section 2.2, the experiments were performed using 3 different size groups to maximize the separation efficiency. A laboratory-scale shaking table (Wilfley, UK) was used in the gravity separation experiments. The experimental conditions were determined according to a previous study (Terzi, 2017) where the shaking table separation of ore with similar physical characteristics was investigated. The variable parameters used for the separations are presented in Table 2. The solids ratio of the pulp (25%), feed rate (6 kg/h), and stroke amplitude (15 mm) parameters were kept constant in all experiments.

A laboratory-scale chamber-type wet high-intensity magnetic separator (Boxmag Rapid, UK) was used in the magnetic separation experiments. The magnetic separation experiments were conducted at different amperage (1A/2A/25A) levels to provide different magnetic intensities (0.22 T / 0.46 T / 1.9 T) for the cleaner and scavenger stages. At the initial stage, the gravity middling was scavenged at a magnetic field intensity of 0.46 T to increase the recovery rate by the attraction of interlocked magnetite-containing particles. Subsequently, the magnetic separation at a magnetic field intensity of 1.9 T was applied on the resulted non-magnetic material to produce a possible feed for quartz/feldspar production. Finally, the magnetic fraction that obtained at the magnetic field intensity of 0.46 T was combined with the gravity concentrate and processed in a cleaner stage at a magnetic field intensity of 0.22 T. To reach the required magnetic field intensity values, 6 grids with 1.5 mm × 3 mm openings were assembled in the separation chamber. Moreover, feeding was realized at a rate of 4 kg/h in a discontinuous manner to prevent clogging in the separation chamber. The solids ratio of the pulp (25%) was kept constant in all experiments.

Table 2. Experimental conditions of gravity separation

Particle Size (mm)	Circuit	Inclination (°)	Stroke (rpm)	Wash Water (dm³/min)
1×0.5	Rougher	8	340	10
	Scavenger	9	370	9
	Cleaner	10	400	8
0.5×0.212	Rougher	7	370	9
	Scavenger	8	400	8
	Cleaner	9	430	7
0.212×0.038	Rougher	6	400	8
	Scavenger	7	430	7
	Cleaner	8	460	6

2.2.3. Zeta potential measurements

The conventional flotation experiments were performed to obtain a final concentrate from the iron-rich heavy mineral pre-concentrate. Zero point of charge (*ZPC*) is a very important feature used to characterize the electrical double layer and the mineral surfaces in flotation. *ZPC* can be used to estimate the charge of mineral surface whether it is positively or negatively charged at a given pH range. *ZPC* values of different minerals in an ore are important in terms of determining the flotation conditions and enabling the effective separation of one mineral from others (Jordens et al., 2013). Thus, the zeta potential values of quartz and magnetite, which are the main gangue and ore minerals within the sample, were measured to establish a route for the flotation experiments.

Since the magnetite-rich concentrate produced as a result of pre-enrichment does not have sufficient purity to be used in zeta potential measurements, the sample was subjected to a magnetic separation

process using a hand-magnet until the non-magnetic minerals in the sample were completely removed (Fig. 2a and b). Additionally, as seen from the *XRD* result of the purified sample shown in Fig. 2c, the sample was purified well enough for the measurements.

2.2.4. Flotation experiments

The conventional flotation experiments were conducted using a set-up consisting of a lab-scale Denver D-12 flotation device and an Orion A211 tabletop pH meter. Reverse anionic and cationic flotation (flotation of silicate minerals from iron concentrate) remains the most popular flotation scheme used in the iron ore industry. While anionic collectors mainly consist of fatty acid, alkyl sulfonic acid, alkyl sulfuric acid, alkyl hydroxamic acid, and sodium or potassium salts, various amines are used as cationic collectors during reverse flotation of iron ores (Cao et al., 2013; Filippov et al., 2014). In the experiments, the reverse flotation method was applied, and according to the results of zeta potential measurements, the applicability of both anionic and cationic flotation schemes was examined. Flotigam *EDA* and NaOl (>82% fatty acids) were used as the collectors in cationic and anionic flotation experiments, respectively. Additionally, MIBC (98%) was used as a frother. $CaCl_2$ (99.9%) was used as a quartz activator in anionic flotation, HCl (37%) and NaOH (>99%) as pH adjusters, and corn starch (25% amylose/75% amylopectin) as an iron depressant in anionic flotation. All of the reagents used in the flotation experiments were purchased from Sigma Aldrich, USA except Flotigam *EDA* (Clariant, Switzerland) and corn starch (Tekkim, Turkey). Moreover, mono-distilled water (*GFL*, Germany) was used in all experiments. The conditions of the anionic and cationic flotation experiments are presented in Table 3.

Table 3. Experimental conditions of flotation experiments

	Variable Conditions		Constant Conditions	
	Anionic Flotation	Cationic Flotation	S/L Ratio (%)	10
pH	11	3	Mixing Speed (rpm)	1000
Collector (g/Mg) – C	500	200	Air Flow Rate (dm^3/min)	10
Frother (g/Mg) – F	500	100	C/D/A Conditioning (min)	5
Depressant (g/Mg) – D	500	-	F Conditioning (min)	1
Activator (g/Mg) – A	500	-	Flotation Time (min)	5

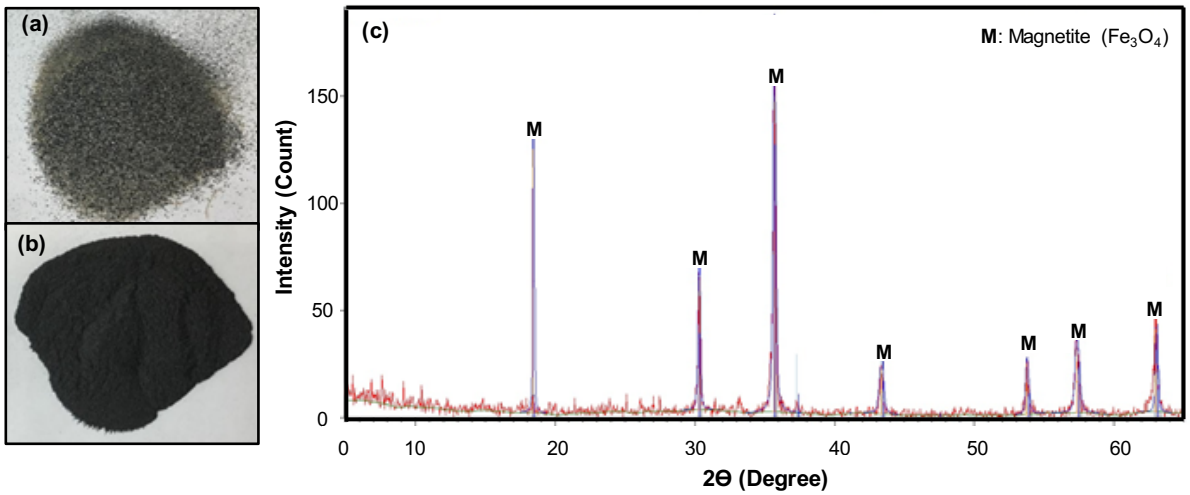

Fig. 2. Purification of magnetite pre-concentrate; (a) before, (b) after, (c) *XRD* result of the purified magnetite sample

2.2.5. Evaluation of experimental results with a digital image processing method

The digital image processing (*DIP*) method, which was successfully applied in the evaluation of processing results of ores that mainly contain minerals with obvious color differences such as feldspar

in previous studies (Ozdemir et al., 2016; Kursun et al., 2018), was used in the determination of mineral contents of the products obtained from flotation experiments, and indirect calculation of recovery rates. In the *DIP* analyzes, the samples were photographed using an optical microscope under appropriate lighting conditions, and the ratio of dark and light-colored minerals in the microscope images was determined by using open-source *ImageJ* software. *ImageJ* is an open-source Java image processing program. 8-bit, 16-bit, and 32-bit images can be analysed and processed in the program (ImageJ, 2020).

The percentage area value obtained after this process represents the cross-sectional area (*CSA*) of the dark minerals in the sample relative to the white minerals. The image processing steps with *ImageJ* are seen in Fig. 3, and the examples of the original and processed images are given in Fig. 4. The analysis procedure performed on the microscope images with 3264x1836 resolution is as follows:

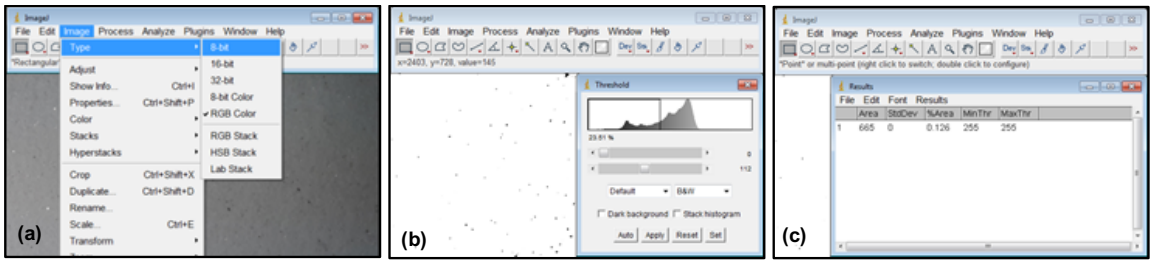

Fig. 3. Cross sectional area calculation with *ImageJ* (a) 8-bit conversion, (b) thresholding; (c) Area % calculation

As a first step, the microscope images were converted to 8-bit grayscale (Image>Type>8-bit) to perform the thresholding (Fig. 3a). The resulting 8-bit images were converted to a 2-color (black and white) by specifying a threshold value (Image>Adjust>Threshold). The threshold value was determined automatically by software in the images of concentrates where dark minerals are predominant, and manually in the images of concentrates where light minerals are predominant to an optimum value where the processed image represents the original image in terms of black and white minerals (Fig. 3b). The ratio of black pixels to white pixels in the 2-color image was calculated using Analyze>Measure. The principle of the measurements is based on the calculation of the ratio of black pixels to white pixels in any given image (Fig. 3c). This procedure was performed on 5 different images taken from the fresh samples of each feed or processed product.

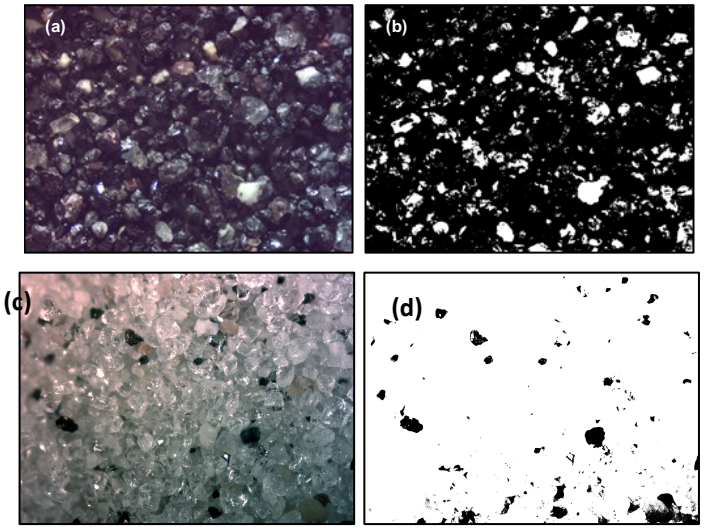

Fig. 4. Examples of (a-c) original images, (b-d) processed images

3. Results and discussion

3.1. Effect of scrubbing on *PSD*

It was determined that the scrubbing process showed a significant effect on the *PSD* of the sample. The ratio of the 1×0.038 mm fraction was increased to 83.69% from 78.92% after the 10-min scrubbing

process. These results showed that the cemented structures were broken down and liberated effectively and particle surfaces were cleaned from the contamination and passed to the slime fraction (-0.038 mm). Although the *PSD* of the samples obtained at the 1st and 5th min of the scrubbing process was similar, the optimum scrubbing time was determined as 10 min as a more prominent change was observed at this duration.

3.2. Gravity separation

The results of gravity separation experiments are shown in Fig. 5. As a result of enrichment with a shaking table, the *CSA* value of 1×0.5 mm fraction was increased to 35.30% from 7.66%. However, the recovery was quite insufficient (~19%). It was determined that the primary reason for this situation can be attributed to the fact that the behavior of the majority of dark-colored minerals was similar to light minerals such as quartz, which were partly inter-locked with dark-colored minerals in this fraction, on the middling and tailing zones of the table. These results revealed that it was not possible to achieve a removal of tailing with a low iron grade, which was the primary goal of pre-enrichment in this fraction, even with the scavenger stage. On the other hand, approximately 400% increment in the *CSA* value of concentrate was a considerable result.

On the other hand, the *CSA* value of 0.5×0.212 mm fraction was increased to 74.83% from 14.48%. Moreover, a much higher recovery (69.58%) compared to the 1×0.5 mm fraction was also obtained. The higher liberation degree of this fraction had a significant effect on the results obtained. On the other hand, it can be said that the target of rejecting a clean residue was reached only partially with the 5.46% *CSA* of final tailings due to the significant amount of locked magnetite particles in this fraction. The grade increase in the concentrate was consistent with the result obtained in the 1×0.5 mm size fraction. Therefore, it can be said that the result obtained with this fraction was more compatible with the aims of the pre-enrichment process owing to significantly higher recovery with a similar upgrade rate.

Finally, the *CSA* value of 0.212×0.038 mm fraction was increased to 83.46% from 13.44% with a recovery rate of approximately 92%. The advantage of the highest particle liberation degree observed in this fraction was positively affected both grade and recovery rate. Therefore, it can be said that the target of obtaining a clean residue was successfully achieved in this fraction with the 1.04% *CSA* of the final tailing. Therefore, an approximately 500% increase in the *CSA* value showed that the gravity separation method can be applied with high success in this particle size fraction.

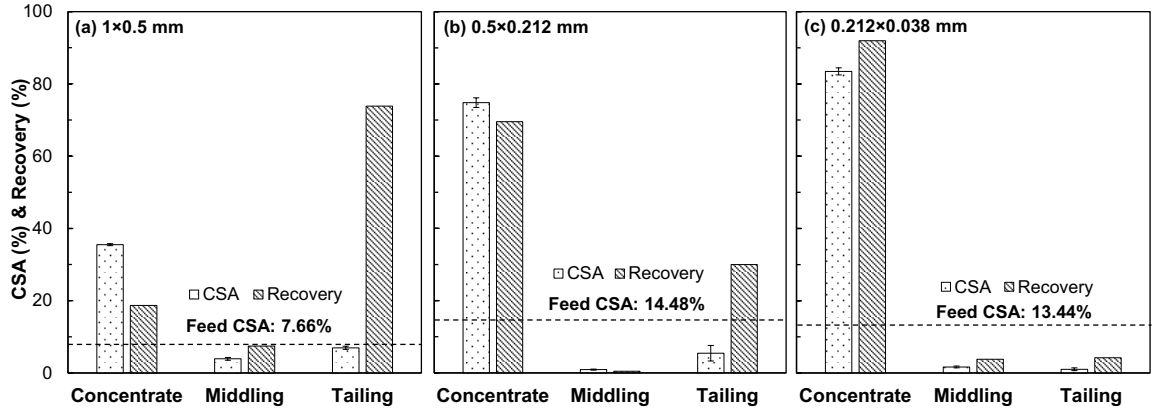

Fig. 5. Results of gravity separation performed on (a) 1×0.5 mm fraction, (b) 0.5×0.212 mm fraction, (c) 0.212×0.038 mm fraction

3.3. Magnetic separation

The results of magnetic separation experiments are seen in Fig. 6. As a result of magnetic separation, the *CSA* value of 1×0.5 mm gravity concentrate was increased from 35.30% to 56.97%. On the other hand, due to the low particle liberation, the recovery rate was not exceeded by 79.72%. The overall recovery obtained in the sequential application of the gravity and magnetic separation process was about 15.61%. Moreover, the *CSA* value of gravity middling was decreased from 3.92% to 2.50% by two-stage magnetic separation applied at 2 A and 25 A. Accordingly, it can be said that the evaluation of the

obtained product from this step as a potential feed sample for quartz/feldspar recovery was a considerable option. The results of both shaking table and magnetic separation experiments clearly showed that a 1×0.5 mm fraction was not suitable to direct processing without any size-reduction process due to its low particle liberation degree.

The *CSA* value of 0.5×0.212 mm gravity concentrate was increased from 74.83% to 84.31% with a recovery rate of 98.89%. Moreover, the overall recovery rate obtained by the sequential application of the gravity and magnetic separation processes was about 69.14%. Additionally, similar to the 1×0.5 mm fraction, the *CSA* value of gravity middling of 0.5×0.212 fraction was decreased from 0.90% to 0.68% after the application of 2 A and 25 A magnetic separation. The obtained results were indicated that both gravity and magnetic separation experiments were effective on 0.5×0.212 fraction in terms of enrichment without a prior comminution process while providing a sufficient recovery rate.

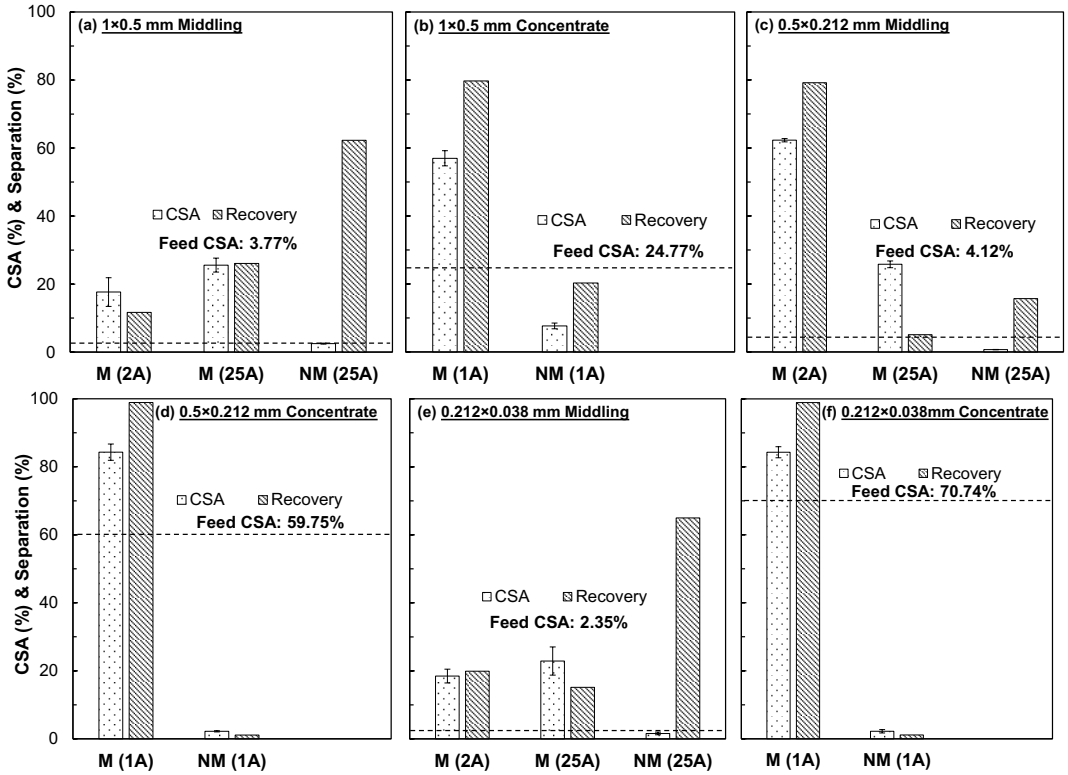

Fig. 6. Results of magnetic separation performed on (a) 1×0.5 mm gravity middling, (b) 1×0.5 mm gravity concentrate, (c) 0.5×0.212 mm gravity middling, (d) 0.5×0.212 mm gravity concentrate, (e) 0.212×0.038 mm gravity middling, (f) 0.212×0.038 mm gravity concentrate

Finally, the *CSA* value of 0.212×0.038 mm gravity concentrate was increased from 83.46% to 88.06% with a recovery rate of 98.55%. On the other hand, the overall recovery rate obtained by the sequential application of the gravity and magnetic separation processes was about 91.35%, which was the highest recovery among all of the size fractions. Additionally, similar to 1×0.5 mm and 0.5×0.212 mm fractions yet in a rather limited manner, the *CSA* value of gravity middling of 0.5×0.212 fraction was decreased from 1.68% to 1.59% after the application of 2 A and 25 A magnetic separation. Accordingly, it can be said that generally the 25 A non-magnetics of all fractions can be used, albeit after grinding of the 1×0.5 mm and 0.5×0.212 fractions due to the low liberation, for feed to a quartz/feldspar recovery. Finally, the obtained results were indicated that both gravity and magnetic separation experiments were effective on 0.212×0.038 fraction in terms of enrichment without a prior comminution process while providing a sufficient recovery rate.

3.4. Zeta potential measurements

In literature, the *ZPC* values of quartz range from 1.7 to 2.6. These differences may arise from the difference in production, storage, and surface properties of the quartz. *ZPC* of quartz can be established

only by extrapolation since it occurs in a low pH range, and the acid side of the curve is not accessible to electrokinetic measurement (El-Salmawy et al., 1993; Bu et al., 2017). On the other hand, the *ZPC* of magnetite values ranged from 3 to 7 (Kosmulski, 2009). Milonjić et al. (1983) stated that the *ZPC* of magnetite decreased to 3.8 after the treatment with HCl due to possible structure changes on the magnetite surface. The zeta potential results of pure quartz and magnetite samples are shown in Fig. 7. The *ZPC* value of the magnetite was determined as approximately 3.8. It was thought that the difference between the obtained *ZPC* value of the magnetite and the values presented in the previous studies might be attributed to the possible alteration of the magnetite samples due to weathering conditions in the ore reserve.

On the other hand, the quartz sample showed a negative surface charge in the examined pH range. However, under high alkaline conditions, the quartz surface charge increased to -60 mV due to the increase in OH- concentration. In the case of extrapolation of the obtained zeta potential profile, it can be seen that the *ZPC* of the quartz will be about pH = 1.8. This result revealed that the obtained zeta potential curve was similar to the typical zeta potential curves of the quartz in literature, and was consistent with previous studies. The surface charges of quartz and magnetite minerals in the range of pH 2 to 4 indicated different markings supported by measurements, and it was determined that the difference between the surface charges of these two minerals reached a maximum level at pH 3. According to these results, two different flotation schemes, namely an anionic flotation scheme using a depressant and an activator and a cationic flotation scheme using only a collector were established.

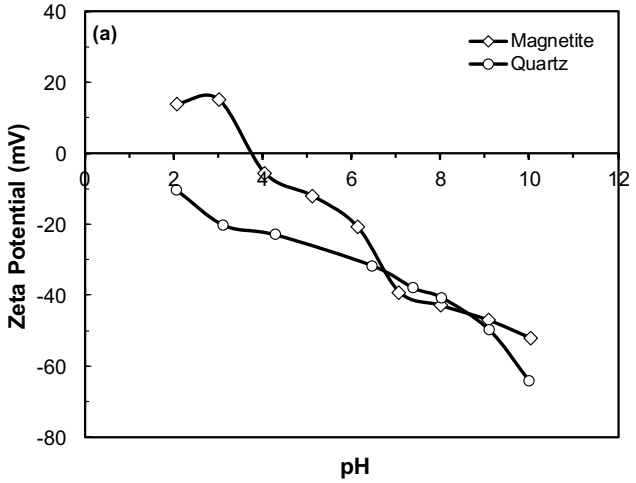

Fig. 7. Zeta potential profiles of magnetite and quartz samples as a function of pH

3.5. Flotation experiments

The anionic reverse flotation experiments using NaOl and $CaCl_2$ and the cationic reverse flotation experiments using Flotigam *EDA* as the collectors were performed to improve the *CSA* values by the removal of the light-colored quartz-rich contents from the concentrate obtained from the sequential gravity-magnetic separation experiments. The *CSA* values of the concentrates obtained from the flotation experiments and the recovery rates calculated based on these values are presented in Fig. 8. As a result of the anionic reverse flotation experiments using NaOl, a slight increase, 84.64% to 84.76%, in the *CSA* value of the concentrate (sinking) was obtained. On the other hand, 1.66% of the dark-colored magnetite-rich content was lost in the tailing (floating) fraction. When the results were analyzed in terms of light-colored quartz-rich fraction removal, it was determined that only 2.58% of the light-colored quartz-rich content in the feed sample could be removed with the anionic reverse flotation using NaOl.

Again, a slight increase, 84.64% to 85.16%, in the *CSA* value of concentrate (sinking) was obtained in the cationic reverse flotation experiments using Flotigam *EDA*. However, 3.71% of the dark-colored magnetite-rich content was lost in the tailing (floating) fraction. When the results were analyzed in terms of the removal of the light-colored quartz-rich fraction by the anionic reverse flotation experiments using Flotigam *EDA*, it was found that 7.54% of the light-colored quartz-rich content in the feed sample could be removed. However, the results obtained with Flotigam *EDA* were relatively higher than those

with NaOl in terms of both the increase in the *CSA* value of the concentrate and light-colored quartz-rich fraction removal.

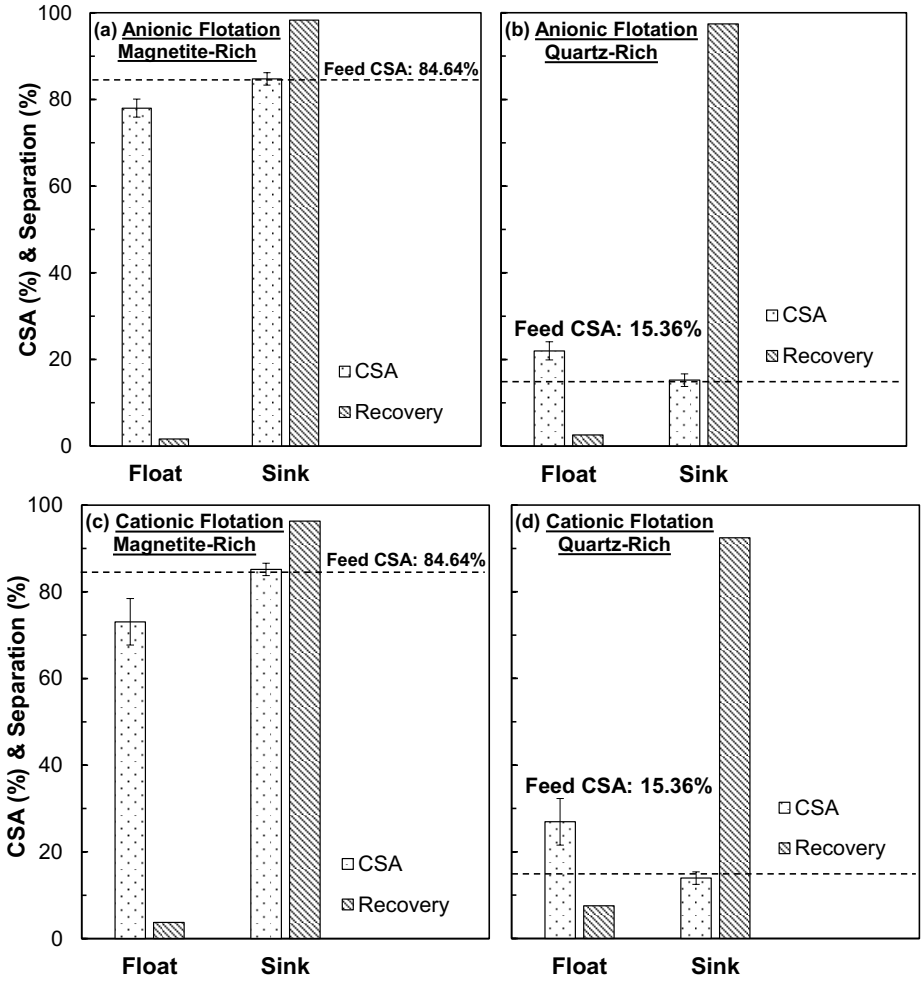

Fig. 8. Effect of flotation experiments on *CSA* and recovery (a) using anionic flotation on dark-colored magnetite rich fraction, (b) using anionic flotation on light-colored quartz-rich fraction, (c) using cationic flotation on dark-colored magnetite rich fraction, (d) using cationic flotation on the light-colored quartz-rich fraction

3.6. Comparison of *DIP* and *ICP* assay values

To determine the reliability and sensitivity of the *CSA* results calculated by the *DIP* method, Fe_2O_3 and TiO_2 grades of the flotation feed sample and cationic flotation concentrate were also analysed using the ICP method, which its details were presented in Section 2.1. Moreover, the *XRD* result of the flotation concentrate, which was conducted to identify iron and titanium-bearing minerals within the final product, is shown in Fig. 9. A comparison of the results for the *DIP* and *ICP* analyzes is presented in Table 4.

Table 4. Comparison of the results for the *DIP* and *ICP*

	DIP/*CSA*	*ICP* (%)		Variation (%)	
	(%)	Fe_2O_3	Fe_2O_3+TiO_2	Fe_2O_3	Fe_2O_3+TiO_2
Flotation Feed	84.64	76.16	85.58	+11.13	-1.10
Flotation Concentrate	85.16	79.13	88.30	+7.62	-3.56

As seen in Table 4 and previously presented, the *CSA* values of the cationic flotation feed and concentrate were calculated as 84.64% and 85.16%, respectively. On the other hand, using the *ICP* method, the Fe_2O_3 grade of the same products were determined as 76.16% and %79.13, respectively.

Therefore, while the slight grade increase with cationic flotation was successfully determined with both methods, the *CSA* values of the samples are higher in both cases than the *ICP* results. These results can be attributed to the fact that the *CSA* values are concurrently represented dark-colored-mafic minerals other than the iron minerals due to limitations of the used methodology.

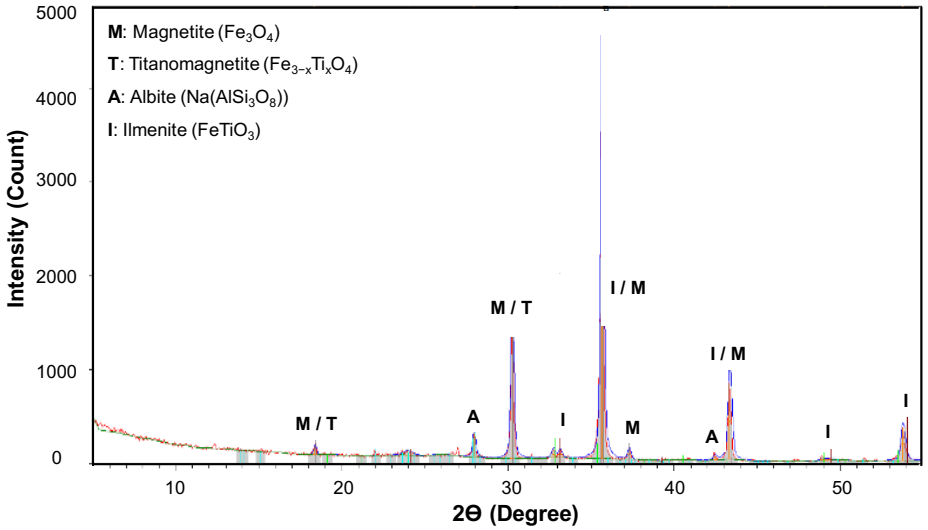

Fig. 9. *XRD* result of the flotation concentrate

In this regard; TiO_2, which is the second-highest content originated from dark colored-opaque minerals was also taken into the consideration and Fe_2O_3+TiO_2 grades were also evaluated. As stated in the results of *XRD* analyzes and optical microscope inspection, TiO_2 content in the sample is mainly associated with ilmenite and titanomagnetite particles, which was confirmed with further inspections carried out on the flotation concentrates. It was found that Fe_2O_3+TiO_2 grades of the flotation feed and concentrate determined by the *ICP* method were 85.58% and 88.30%, respectively, which were very close to and only negatively variated in the range 1.10-3.56% from the *CSA* values. Therefore, it can be said that the simultaneous evaluation of *ICP* results of Fe_2O_3+TiO_2 correlates better with the calculated *CSA* values than the former option, where the only Fe_2O_3 grade is taken into consideration. Hence, the application of a correlation coefficient derived from these results would be sufficient in terms of an accurate representation of the Fe_2O_3 grades.

Gulcan and Gulsoy (2017) have pointed out that optical sorting, which is a method based on DIP, of quartz and magnesite samples were resulted in high sorting efficiencies due to fact that both samples having high color contrast among their particles. On the other hand, it was also stated that the same separation method arose some challenges for the samples that have moderate color-contrast (lignite and hematite) and low color contrast (copper and gold). Sousa et al. (2020) have also stated that the optical sorting of a coarse-grained fraction of a Li-Mica lepidolite ore would be feasible due to the high-contrast between valuable and non-valuable particles and the optical separator performance become lower when color contrast decreases. Similar to these examples, the high contrast requirement is the main limitation of the procedure presented in this work in terms of a successful application.

Finally, these results showed that the *DIP* analysis can be successfully used for the determination of dark-colored mineral ratios and grades in the iron concentrate production from silica-rich river sediment or other similar ores, where a distinct color difference is present between the valuable and gangue minerals.

4. Summary and Conclusions

In this study, the possibility of iron-rich heavy mineral concentrate production from silica-rich river sediment with SiO_2 and Fe_2O_3 contents of 59.16% and 6.82%, respectively, obtained from the Canakkale region of Turkey, by gravity, magnetic separation, and flotation methods were investigated. The mineral processing experiments were carried out by using a laboratory scale Wilfley type shaking table,

a wet high-intensity chamber type magnetic separator, and a Denver flotation cell on the 1×0.5, 0.5×0.212, and 0.212×0.038 mm fractions of the head sample. The *DIP* method was used to determine the mineral content of the products obtained from enrichment experiments and indirect calculation of the recovery rates. The results of the *DIP* analyzes showed that it was possible to successfully determine the dark-colored mineral ratios and grades in the iron-rich heavy mineral concentrate production from a silica-rich river by the application of the investigated methodology with a correlation coefficient derived from the obtained results. However, it should be noted that the DIP analyzes solely based on color/contrast differences have their limitations due to the necessity of a distinct contrast/color difference between the minerals within an ore. Therefore, the applicability of the procedure presented in our work should be separately evaluated for the analyzes of different ore types, especially for the ores that have limited contrast/color difference between the ore/gangue minerals.

As a result of the gravity and magnetic separation, it was determined that the production of concentrate with the *CSA* value of 84.64% from the 1×0.5 mm, 0.5×0.212, and 0.212×0.038 size fractions can be achieved under the conditions investigated. Additionally, it was also determined that a 1×0.5 mm size fraction should be enriched after a grinding stage due to the insufficient liberation degree of the fraction.

In the flotation experiments, an increase in *CSA* values of concentrates was slight in both anionic and cationic flotation schemes, as a result of the low amount of quartz-rich fraction floating due to difficulties encountered in froth formation and stability. After the cationic flotation, *CSA* values of the final concentrate and general recovery rate of iron-rich heavy mineral fraction were calculated as 85.16% (79.13% Fe_2O_3) and 57.81%, respectively. The chemical composition of the final iron-rich heavy mineral concentrate and quartz-rich silicate concentrates are given in Table 5.

Table 5. Chemical analysis results of the final iron and silicate concentrates

Oxides	Assay Values (%)	
	Iron Concentrate	Silicate Concentrate
Al_2O_3	2.88	22.26
Fe_2O_3	79.13	0.23
K_2O	0.12	1.06
CaO	0.41	6.01
MgO	0.97	0.09
Na_2O	0.31	6.96
P_2O_5	0.40	Not Detected
SiO_2	5.53	62.48
TiO_2	9.17	0.00*
LOI	0.54	0.32

As seen in Table 5, the iron grade of the final concentrate is rather low for conventional iron production processes. However, several studies have shown that the low-grade (27-45% Fe) iron ores can be utilized in iron processing by alternative pre-processing strategies such as smelting after pelletizing with coal and bentonite (Srivastava and Kawatra, 2009) or reduction roasting (Ray et al., 2018), then the applying a LIMS step for both processes. Additionally, there are several direct smelting technologies have been applied in the iron smelting industry for different low-grade iron materials, albeit with several advantages or disadvantages (Anameric and Kawatra, 2008).

The results obtained in this study show that it is possible to produce both an iron-rich heavy mineral concentrate and a potential feed for the production of quartz sand and feldspar concentrates from the ore with the application of the flow chart given in Fig. 9. However, the investigation of the removal possibilities SiO_2, Al_2O_3, TiO_2, and other impurities (Table 5), in terms of the evaluation of the suitability of the concentrate for iron production processes is recommended for further studies. Additionally, a quartz/feldspar separation with flotation seems to be necessary as the silicate concentrate contains a significant amount of feldspar mineral in addition to the quartz content. Finally, further investigations of the causes and possible solutions to the difficulties encountered in froth formation and stability are also recommended.

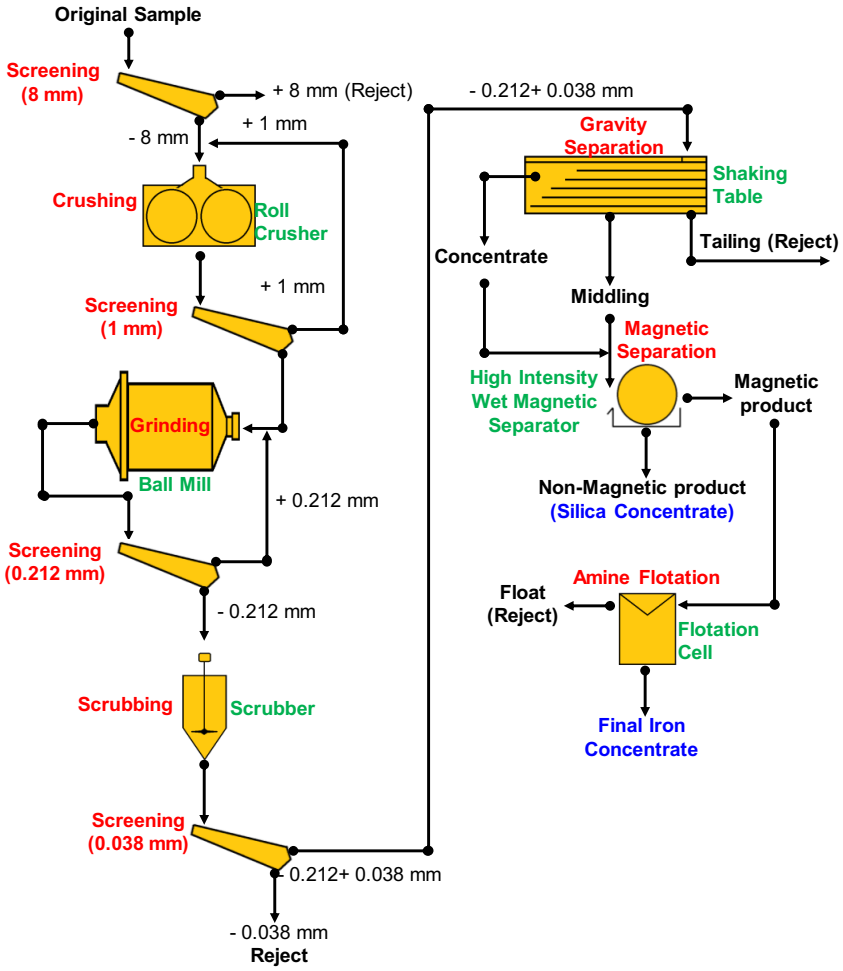

Fig. 9. Proposed simplified flow chart for a possible scale-up

Acknowledgments

This work was supported by Scientific Research Projects Coordination Unit of Istanbul University-Cerrahpasa, Project number 26084.

References

ALDRICH, C., MARAIS, C., SHEAN, B.J., CILLIERS, J.J., 2010. *Online monitoring and control of froth flotation systems with machine vision: A review.* Int. J. Miner. Process. 96, 1-13.

ANAMERIC, B., KAWATRA, S.K., 2008. *Direct iron smelting reduction processes*. Miner. Process. Extr. Metall. Rev. 30, 1-51.

BHARGAVA, O.P., 2006. *Iron Ore, Sample Preparation and Analysis of.* In: Meyers, R.A., (eds.) Encyclopedia of Analytical Chemistry: Applications, Theory and Instrumentation. Wiley.

BILLINGSLEY, F.C., 1970. *Applications of digital image processing.* Appl. Opt. 9, 289-299.

BU, X., EVANS, G., XIE, G., PENG, Y., ZHANG, Z., NI, C., GE, L., 2017. *Removal of fine quartz from coal-series kaolin by flotation.* Appl. Clay Sci. 143, 437-444.

CAO, L., 2006. *Singular value decomposition applied to digital image processing.* Division of Computing Studies, Arizona State University Polytechnic Campus, Mesa, Arizona State University Polytechnic Campus.

CAO, Z., ZHANG, Y., CAO, Y., 2013. *Reverse flotation of quartz from magnetite ore with modified sodium oleate*. Miner. Process. Extr. Metall. Rev. 34, 320-330.

CHRISTIE, T., BRATHWAITE, B., 1997. *Mineral commodity report 15 – Iron*. NZ Min 22, 22-37.

DEATH, D.L., CUNNINGHAM, A.P., POLLARD, L.J., 2008. *Multi-element analysis of iron ore pellets by laser-induced breakdown spectroscopy and principal components regression*. Spectrochim. Acta B 63, 763-769.

EL-SALMAWY, M.S., NAKAHIRO, Y., WAKAMATSU, T., 1993. *The role of alkaline earth cations in flotation separation of quartz from feldspar.* Miner. Eng. 6, 1231-1243.

ENDO, Y., SAKAO, N., 1980. *Application of High-frequency Inductively Coupled Plasma Emission Spectrometry to Analysis of Iron Ores.* Tetsu-to-Hagane 66, 1395-1400.

FILIPPOV, L.O., SEVEROV, V.V., FILIPPOVA, I.V., 2014. *An overview of the beneficiation of iron ores via reverse cationic flotation.* Int. J. Miner. Process. 127, 62-69.

GULCAN, E., GULSOY, O.Y., 2017. *Performance evaluation of optical sorting in mineral processing–A case study with quartz, magnesite, hematite, lignite, copper and gold ores*. Int. J. Miner. Process. 169, 129-141.

HACIFAZLIOGLU, H., 2011. *Methods used in the beneficiation of silica sand and comparison of flotation and magnetic separation in terms of iron removal.* Scientific Mining Journal 50, 35-48.

IMAGE J., 2020. *ImageJ.* http://rsb.info.nih.gov/ij/ (Accessed 02 October 2020).

JORDENS, A., CHENG, Y.P., WATERS, K.E., 2013. *A review of the beneficiation of rare earth element bearing minerals.* Miner. Eng. 41, 97-114.

KHORRAM, F., MEMARIAN, H., TOKHMECHI, B., SOLTANIAN-ZADEH, H., 2011. *Limestone chemical components estimation using image processing and pattern recognition techniques.* Journal of Mining and Environment 2, 126-135.

KOSE, M., TURELI, T. K., 1986. *The required properties of the quartz sands for glass making and their beneficiation methods and a case study of Yozgat Sarikaya quartzites.* Scientific Mining Journal 25, 21-28.

KOSMULSKI, M., 2009. *Surface charging and points of zero charge.* CRC Press, Florida, USA.

KURSUN, I., 2009. *Particle size and shape characteristics of Kemerburgaz quartz sands obtained by sieving, laser diffraction, and digital image processing methods.* Miner. Process. Extr. Metall. Rev. 30, 346-360.

KURSUN, I., TERZI, M., OZDEMIR, O., 2018. *Evaluation of digital image processing (DIP) in analysis of magnetic separation fractions from Na-feldspar ore.* Arab. J. Geosci. 11, 462.

LI, C., SUN, H., BAI, J., LI, L., 2010. Innovative methodology for comprehensive utilization of iron ore tailings: Part 1. The recovery of iron from iron ore tailings using magnetic separation after magnetizing roasting. J. Hazard. Mater. 174, 71-77.

LIU, S., ZHAO, Y., WANG, W., WEN, S. 2014. *Beneficiation of a low-grade, hematite-magnetite ore in China.* Miner. Metall. Process. 31, 136-142.

MARAS, H.H., MARAS, S.S., YILDIZ, F., 2010. *An overview of medical image processing methods.* Afr. J. Biotechnol. 9, 3666-3675.

MILONJIĆ, S.K., KOPEČNI, M.M., ILIĆ, Z.E., 1983. *The point of zero charge and adsorption properties of natural magnetite.* J. Radioanal. Nucl. Chem. 78, 15-24.

MOOLMAN, D.W., ALDRICH, C., VAN DEVENTER, J.S.J., STANGE, W.W., 1994. *Digital image processing as a tool for on-line monitoring of froth in flotation plants.* Miner. Eng. 7, 1149-1164.

OZDEMIR, O., KURSUN UNVER, I., TERZI, M., YILMAZ, K., 2016. *An investigation of digital image processing (DIP) method for analysis of grade of feldspar ore based on color differences*. In: Bascetin, A., Kursun, I., Ozdemir, O. (eds.) Proceedings of 6th International Conference on Computer Applications in the Minerals Industries, 55, 1-4.

PEREZ, C.A., ESTÉVEZ, P.A., VERA, P.A., CASTILLO, L.E., ARAVENA, C.M., SCHULZ, D.A., MEDINA, L.E., 2011. *Ore grade estimation by feature selection and voting using boundary detection in digital image analysis.* Int. J. Miner. Process. 101, 28-36.

RAHMAN, M.A., ZAMAN, M.N., BISWAS, P.K., SULTANA, S., NANDY, P.K., 2015. *Physical separation for upgradation of valuable minerals: A study on sands of the Someswari river.* Bangladesh Journal of Scientific and Industrial Research 50, 53-58.

RAJIB, M., ZAMAN, M.M., KABIR, M.Z., DEEBA, F., RANA, S.M., 2009. *Physical upgradation and characterization of river silica of Bangladesh to be used as glass sand.* In: Proceedings of International Conference on Geoscience for Global Development, 192-196.

RAY, N., NAYAK, D., DASH, N., RATH, S.S., 2018. *Utilization of low-grade banded hematite jasper ores: recovery of iron values and production of ferrosilicon*. Clean Technol. Envir. 20, 1761-1771.

SEIFELNASSR, A.A., MOSLIM, E.M., ABOUZEID, A.Z.M., 2013. *Concentration of a Sudanese low-grade iron ore.* Int. J. Miner. Process. 122, 59-62.

SHENG, L., ZHANG, T., WANG, K., TANG, H., LI, H., 2015. *Quantitative analysis of Fe content in iron ore via external calibration in conjunction with internal standardization method coupled with LIBS.* Chem. Res. Chin. Univ. 31, 107-111.

SINGH, V., RAO, S.M., 2006. *Application of image processing in mineral industry: a case study of ferruginous manganese ores.* Miner. Process. Extr. Metall. Rev. 115, 155-160.

SOUSA, R., FUTURO, A., FIÚZA, A., LEITE, M.M., 2020. *Pre-concentration at crushing sizes for low-grade ores processing–Ore macro texture characterization and liberation assessment.* Miner. Eng. 147.

SRIVASTAVA, U., KAWATRA, S.K., 2009. *Strategies for processing low-grade iron ore minerals*. Miner. Process. Extr. Metall. Rev. 30, 361-371.

STANFORD, R.L., MEREDITH, D.L., SPEARS, D.R., 1992. *Computer vision applications in mineral processing research.* In: Conference Record of the 1992 IEEE Industry Applications Society Annual Meeting, 2013-2019.

TERZI, M., 2017. *Development of new processes for beneficiation of Isparta region rare earth elements.* Ph.D. Thesis, Istanbul University, Istanbul, Turkey.

UBALDINI, S., PIGA, L., FORNARI, P., MASSIDDA, R., 1996. *Removal of iron from quartz sands: A study by column leaching using a complete factorial design.* Hydrometallurgy 40, 369-379.